

A magnetar giant flare in the nearby starburst galaxy M82

Sandro Mereghetti^{1,*}, Michela Rigoselli¹, Ruben Salvaterra¹, Dominik Patryk Pacholski^{1,2}, James Craig Rodi³, Diego Gotz⁴, Edoardo Arrigoni^{5,1}, Paolo D’Avanzo⁶, Christophe Adami⁷, Angela Bazzano³, Enrico Bozzo^{8,6}, Riccardo Brivio^{9,6}, Sergio Campana⁶, Enrico Cappellaro¹⁰, Jerome Chenevez¹¹, Fiore De Luise¹², Lorenzo Ducci^{13,8}, Paolo Esposito^{14,1}, Carlo Ferrigno^{8,6}, Matteo Ferro^{9,6}, Gian Luca Israel¹⁵, Emeric Le Floc’h⁴, Antonio Martin-Carrillo¹⁶, Francesca Onori¹², Nanda Rea^{17,18}, Andrea Reguitti^{6,10}, Volodymyr Savchenko¹⁹, Damyia Souami²⁰, Leonardo Tartaglia¹², William Thuillot²¹, Andrea Tiengo^{14,1}, Lina Tomasella¹⁰, Martin Topinka²², Damien Turpin⁴, Pietro Ubertini³

¹*INAF - Istituto di Astrofisica Spaziale e Fisica Cosmica di Milano, Via A. Corti 12, 20133 Milano, Italy*

²*Università degli Studi di Milano Bicocca, Dipartimento di Fisica G. Occhialini, Piazza della Scienza 3, 20126 Milano, Italy*

³*INAF - Istituto di Astrofisica e Planetologia Spaziali di Roma, Via del Fosso del Cavaliere 100, 00133 Roma, Italy*

⁴*Université Paris-Saclay, Université Paris Cité, CEA, CNRS, AIM, 91191, Gif-sur-Yvette, France*

⁵*Università degli Studi di Milano, Dipartimento di Fisica, Via Celoria 16, 20133 Milano, Italy*

⁶*INAF - Osservatorio Astronomico di Brera, Via E. Bianchi 46, 23807 Merate, Italy*

⁷*Aix Marseille Univ, CNRS, CNES, LAM, Marseille, France*

⁸*University of Geneva, Department of Astronomy, Chemin d’Ecogia 16, Versoix 1290, Switzerland*

⁹*Università dell’Insubria, Dipartimento di Scienza e Alta Tecnologia, Via Valleggio 11, 22100 Como, Italy*

¹⁰*INAF - Osservatorio Astronomico di Padova, Vicolo dell’Osservatorio 5, 35122 Padova, Italy*

¹¹*DTU Space, Technical University of Denmark, Elektrovej 327, 2800 Kongens Lyngby, Denmark*

¹²*INAF - Osservatorio Astronomico d’Abruzzo, Via M. Maggini snc, 64100 Teramo, Italy*

¹³*Institut fuer Astronomie und Astrophysik Tuebingen, Sand 1, Tuebingen, Germany*

¹⁴*Scuola Universitaria Superiore IUSS Pavia, Piazza della Vittoria 15, 27100 Pavia, Italy*

¹⁵*INAF - Osservatorio Astronomico di Roma, 00078 Monte Porzio Catone, Italy*

¹⁶*School of Physics and Centre for Space Research, University College Dublin, Belfield, Dublin 4, Dublin, Ireland*

¹⁷*Institute of Space Sciences (CSIC-ICE), Campus UAB, Carrer de Can Magrans s/n, 08193 Barcelona, Spain*

¹⁸*Institut d’Estudis Espacials de Catalunya (IEEC), Carrer Gran Capità 2–4, 08034 Barcelona, Spain*

¹⁹*École polytechnique fédérale de Lausanne, Lausanne, Switzerland.*

²⁰*LESIA, Observatoire de Paris, Université PSL, CNRS, Sorbonne Université, Université de Paris, 5 place*

Jules Janssen, F-92195 Meudon, France

²¹ Institut de mécanique céleste et de calcul des éphémérides (IMCCE) UMR 8028 du CNRS - Observatoire de Paris 77 Av. Denfert Rochereau 75014 Paris, France

²² INAF - Osservatorio Astronomico di Cagliari, Via della Scienza 5, 09047 Selargius (CA), Italy

* Corresponding author: sandro.mereghetti@inaf.it

Giant flares, short explosive events releasing up to 10^{47} erg of energy in the gamma-ray band in less than one second, are the most spectacular manifestation of magnetars, young neutron stars powered by a very strong magnetic field, 10^{14-15} G in the magnetosphere and possibly higher in the star interior^{1,2}. The rate of occurrence of these rare flares is poorly constrained, as only three have been seen from three different magnetars in the Milky Way^{3,4} and in the Large Magellanic Cloud⁵ in ~ 50 years since the beginning of gamma-ray astronomy. This sample can be enlarged by the discovery of extragalactic events, since for a fraction of a second giant flares reach peak luminosities above 10^{46} erg s⁻¹, which makes them visible by current instruments up to a few tens of Mpc. However, at these distances they appear similar to, and difficult to distinguish from, regular short gamma-ray bursts (GRBs). The latter are much more energetic events, 10^{50-53} erg, produced by compact binary mergers and originating at much larger distances⁶. Indeed, only a few short GRBs have been proposed⁷⁻¹¹, with different levels of confidence, as magnetar giant flare candidates in nearby galaxies. Here we report the discovery of a short GRB positionally coincident with the central region of the starburst galaxy M82¹². Its spectral and timing properties, together with the limits on its X-ray and optical counterparts obtained a few hours after the event and the lack of an associated gravitational wave signal, qualify with high confidence this event as a giant flare from a magnetar in M82.

Instruments on board the *INTEGRAL* satellite detected GRB 231115A on 2023 November 15 at 15:36:20.7 UT¹³. This short burst (duration $T_{90} = 93$ ms) was seen also by other satellites¹⁴⁻¹⁸, but only *INTEGRAL* could promptly associate it to M82 thanks to a localization at few arcmin level, publicly distributed by the *INTEGRAL* Burst Alert System (IBAS¹⁹) only 13 s after the burst detection. The burst occurred in the field of view of the IBIS coded mask instrument²⁰, at coordinates R.A.=149.0205 deg, Dec.=+69.6719 deg (J2000, 2 arcmin 90% c.l. radius). This position is consistent with, and supersedes, the one derived using the preliminary satellite attitude available in near real time¹³. The position of GRB 231115A coincides with the nearby starburst

galaxy M82¹² (see Figure 1). Notably, the central region of the galaxy, where most star formation activity occurred, is inside the *INTEGRAL*/IBIS error region. Considering that the total angular size of all the galaxies with apparent luminosity brighter than M82 (excluding the Magellanic Clouds and M31) is ~ 6000 arcmin², the chance alignment with GRB 231115A is 4×10^{-5} . A more elaborate analysis²¹ indicates that the Bayes factor favouring a giant flare in M82 with respect to a chance alignment of a short GRB in the background is a factor 30 larger than that of the previous best candidate (GRB 200415A possibly associated to NGC 253⁹), making GRB 231115A by far the most compelling case for a magnetar giant flare outside the local group of galaxies.

The light curves plotted in Figure 2 show that GRB 231115A was clearly visible in the two IBIS detectors, which operate in different energy ranges: ISGRI²² (20 keV – 1 MeV) and PICsIT²³ (175 keV – 15 MeV). The ISGRI and PICsIT spectra of the burst, extracted from the time interval with a significant detection in both detectors (from $T_0+0.687$ s to $T_0+0.748$ s, with $T_0=15:36:20.0$ UT), have been jointly fit and are well described by an exponentially cut-off power law with photon index $\alpha = 0.04_{-0.24}^{+0.27}$, peak energy $E_p = 551_{-59}^{+81}$ keV, and flux $F_{30-2600} = (7.2_{-0.7}^{+0.6}) \times 10^{-6}$ erg cm⁻² s⁻¹ in the 30 keV – 2.6 MeV range (see Methods sect. 1). Assuming this spectral shape for the whole duration of the burst, the fluence in the same energy range is $(6.3 \pm 0.5) \times 10^{-7}$ erg cm⁻².

M82 was in the field of view of IBIS starting from 9.2 hours before up to 11.8 minutes after the burst, as well as during a target of opportunity (ToO) observation performed in the following three days, but no other bursting or persistent emission besides GRB 231115A was detected. Integrating all the data of the ToO observation, we obtained an upper limit of 2.6×10^{-11} erg cm⁻² s⁻¹ on the 30–100 keV persistent emission at the position of GRB 231115A. Also, no other bursts from M82 were detected in all the available ISGRI archival data obtained since 2003, which provided a total exposure of more than 16 Ms (see Methods sect. 1).

At the distance of M82 (3.6 Mpc²⁴), the GRB 231115A fluence measured with IBIS implies an emitted isotropic energy $E_{\text{iso}} = 10^{45}$ erg (1 keV – 10 MeV), well below the typical value for a short GRB, but consistent with the one of the initial pulses of the three giant flares securely associated with magnetars³⁻⁵. The short duration and hard spectrum of GRB 231115A are also in agreement with the properties seen in the initial pulses of magnetar giant flares. In the three giant flares securely associated with magnetars, the initial short and hard pulse was followed by a softer

tail, with a duration of a few minutes and a maximum luminosity of $\sim 10^{42}$ erg s $^{-1}$, characterized by a periodic modulation induced by the neutron star rotation. A similar feature would be too faint to be visible by IBIS at the distance of M82. This is shown in Figure 3, where we compare the limits obtained for GRB 231115A with the light curve of the most energetic Galactic giant flare ever observed (the one emitted by SGR 1806–20 in 2004⁴) rescaled to a distance of 3.6 Mpc.

The field of GRB 231115A was promptly observed with the Neil Gehrels Swift Observatory starting 9 ks after the burst²⁵ and a deeper X-ray observation was carried out with the *XMM-Newton* satellite, starting 0.7 days after the burst²⁶ (see Methods sect. 2). The comparison of the *Swift* and *XMM-Newton* images with those obtained in previous observations of M82 does not show evidence for new X-ray sources inside the GRB 231115A error region. Due to the presence of unresolved X-ray emission from the central part of the galaxy, the corresponding upper limit is position-dependent. The limit of 4×10^{-14} erg cm $^{-2}$ s $^{-1}$ derived from the *XMM-Newton* data, which applies to 60% of the error region, is inconsistent with the flux at T₀+1 day of the large majority of X-ray afterglows of short GRBs detected with the *Swift*/XRT instrument (see Methods Figure 7). Although we can not exclude a rapid afterglow drop, as observed in the class of so-called short lived short GRBs²⁷, this X-ray upper limit disfavors the GRB interpretation. It is instead consistent with the quiescent X-ray emission of a magnetar in M82. In fact the X-ray luminosity of known magnetars, also considering the peak values reached during outbursts²⁸, never exceeds 10^{36} erg s $^{-1}$, corresponding to 6×10^{-16} erg cm $^{-2}$ s $^{-1}$ at the M82 distance.

Holding true the association of GRB 231115A with M82 on the basis of the remarkable spatial coincidence, the low value of E_{iso} could be reconciled with a short GRB origin only if the jet axis is pointed away from our direction, similar to the case of the gravitational wave event GRB 170817A²⁹, which produced the bright kilonova AT2017gfo in the optical/NIR band. However, the deep upper limits of $m > 20.0 - 24.0$ mag (depending on the assumed position in the *INTEGRAL* error circle) on the optical counterpart that we obtained starting at T₀+0.2 days (see Methods sect. 3) exclude this possibility, both for an AT2017gfo-like event and for even fainter kilonovae (see Methods sect. 3). We finally note that the binary merger of two compact objects at 3.6 Mpc would have produced a strong signal in gravitational waves, at variance with the non-detection reported by the LIGO/Virgo/KAGRA Collaboration³⁰.

The discovery of a young, active magnetar in M82, a starburst galaxy characterized by a

high star formation rate³¹ is consistent with the origin of magnetars in core collapse supernova explosions³². The volumetric rate of giant flares with $E_{\text{iso}} > 4 \times 10^{44}$ erg has been recently estimated¹⁰ as $(3.8_{-3.1}^{+4.0}) \times 10^5 \text{ Gpc}^{-3} \text{ yr}^{-1}$. Assuming a direct link with the young stellar population of core collapse progenitors and considering the total star formation rate of $4000 M_{\odot} \text{ yr}^{-1}$ within 50 Mpc, this corresponds to a rate of $R(E_{\text{iso}} > 4 \times 10^{44}) = 0.05_{-0.04}^{+0.05} \text{ yr}^{-1} (M_{\odot} \text{ yr}^{-1})^{-1}$. Given the star formation rate of $7.1 M_{\odot} \text{ yr}^{-1}$ in M82³¹ and assuming a power-law distribution of the giant flares energies with slope 1.7, the expected rate of giant flares with $E_{\text{iso}} > 10^{45}$ erg in M82 is $R_{\text{M82}}(E_{\text{iso}} > 10^{45}) = 0.19_{-0.15}^{+0.19} \text{ yr}^{-1}$. Recent calculations based on relativistic hydrodynamical simulations³³ show that such ejecta are efficient sources for the nucleosynthesis of heavy elements through the r-process. Thus the giant flares with $E_{\text{iso}} > 10^{46}$ erg (each producing up to 10^{26} g of ejecta) can give a yield of $\sim 2 \times 10^{-9} M_{\odot} \text{ yr}^{-1}$ of r-process elements in M82 through this channel.

GRB 051103 is another short GRB that has been proposed as a possible magnetar giant flare in the M81 group of galaxies⁷. According to a detailed statistical analysis¹⁰, M82 is the most likely host of GRB 051103, despite being slightly outside its 260 arcmin² localization region. The rate of giant flares derived above is fully consistent with the detection of two events from M82 in 20 years. Therefore, starburst galaxies such as M82, which produce a significant population of young magnetars, appear as promising targets to constrain the energy distribution function of giant flares by means of long dedicated observations with future high sensitivity instruments.

References

1. Mereghetti, S. The strongest cosmic magnets: soft gamma-ray repeaters and anomalous X-ray pulsars. *Astron. Astrophys. Rev.*, **15**, 225 (2008).
2. Kaspi, V. M., & Beloborodov, A. M. Magnetars. *Annual Review of Astronomy and Astrophysics*, **55**, 261 (2017).
3. Hurley, K., et al. A giant periodic flare from the soft γ -ray repeater SGR1900+14. *Nature*, **397**, 41 (1999).
4. Palmer, D. M., et al. A giant γ -ray flare from the magnetar SGR 1806-20. *Nature*, **434**, 1107 (2005).

5. Mazets, E. P., Golentskii, S. V., Ilinskii, V. N., Aptekar, R. L., & Guryan, I. A. Observations of a flaring X-ray pulsar in Dorado. *Nature*, **282**, 587 (1979).
6. D'Avanzo, P. Short gamma-ray bursts: A review. *Journal of High Energy Astrophysics*, **7**, 73 (2015).
7. Frederiks, D. D., et al. On the possibility of identifying the short hard burst GRB 051103 with a giant flare from a soft gamma repeater in the M81 group of galaxies. *Astronomy Letters*, **33**, 19 (2007).
8. Mazets, E. P., et al. A Giant Flare from a Soft Gamma Repeater in the Andromeda Galaxy (M31). *Astrophys. J.*, **680**, 545 (2008).
9. Svinkin, D., et al. A bright γ -ray flare interpreted as a giant magnetar flare in NGC 253. *Nature*, **589**, 211 (2021).
10. Burns, E., et al. Identification of a Local Sample of Gamma-Ray Bursts Consistent with a Magnetar Giant Flare Origin. *Astrophys. J. Lett.*, **907**, L28 (2021).
11. Trigg, A. C., et al. GRB 180128A: A Second Magnetar Giant Flare Candidate from the Sculptor Galaxy. *arXiv e-prints*, arXiv:2311.09362 (2023).
12. Förster Schreiber, N. M., Genzel, R., Lutz, D., & Sternberg, A. The Nature of Starburst Activity in M82. *Astrophys. J.*, **599**, 193 (2003).
13. Mereghetti, S., et al. GRB 231115A: a short hard GRB detected by IBAS, poitionally coincident with M82. *GRB Coordinates Network*, **35037**, 1 (2023).
14. Dalessi, S., Roberts, O. J., Veres, P., Meegan, C., & Fermi Gamma-ray Burst Monitor Team GRB 231115A: Fermi Observations of a probable Magnetar Giant Flare from M82. *GRB Coordinates Network*, **35044**, 1 (2023).
15. Cheung, C. C., et al. GRB 231115A (short): Glowbug gamma-ray detection. *GRB Coordinates Network*, **35045**, 1 (2023).
16. Xue, W. C., Xiong, S. L., Li, X. B., Li, C. K., & Insight-HXMT Team GRB 231115A: Insight-HXMT/HE detection. *GRB Coordinates Network*, **35060**, 1 (2023).

17. Frederiks, D., et al. Konus-Wind detection of GRB 231115A (a probable Magnetar Giant Flare from M82). *GRB Coordinates Network*, **35062**, 1 (2023).
18. Wang, Y., et al. Study the origin of GRB 231115A, short gamma-ray burst or magnetar giant flare?. *arXiv e-prints*, arXiv:2312.02848 (2023).
19. Mereghetti, S., Götz, D., Borkowski, J., Walter, R., & Pedersen, H. The INTEGRAL Burst Alert System. *Astron. Astrophys.*, **411**, L291 (2003).
20. Ubertini, P., et al. IBIS: The Imager on-board INTEGRAL. *Astron. Astrophys.*, **411**, L131 (2003).
21. Burns, E. GRB 231115A: significance of INTEGRAL localization alignment with M82. *GRB Coordinates Network*, **35038**, 1 (2023).
22. Lebrun, F., et al. ISGRI: The INTEGRAL Soft Gamma-Ray Imager. *Astron. Astrophys.*, **411**, L141 (2003).
23. Labanti, C., et al. The Ibis-Picst detector onboard Integral. *Astron. Astrophys.*, **411**, L149 (2003).
24. Freedman, W. L., et al. The Hubble Space Telescope Extragalactic Distance Scale Key Project. I. The Discovery of Cepheids and a New Distance to M81. *Astrophys. J.*, **427**, 628 (1994).
25. Osborne, J. P., et al. GRB 231115A: Swift-XRT and Swift-UVOT observations. *GRB Coordinates Network*, **35064**, 1 (2023).
26. Rigoselli, M., Pacholski, D. P., Mereghetti, S., Salvaterra, R., & Campana, S. GRB 231115A: XMM-Newton observation. *GRB Coordinates Network*, **35175**, 1 (2023).
27. Sakamoto, T., & Gehrels, N. Indication of Two Classes in the Swift Short Gamma-Ray Bursts from the XRT X-Ray Afterglow Light Curves. *Gamma-ray Burst: Sixth Huntsville Symposium*, **1133**, 112 (2009).
28. Coti Zelati, F., Rea, N., Pons, J. A., Campana, S., & Esposito, P. Systematic study of magnetar outbursts. *Mon. Not. R. Astron. Soc.*, **474**, 961 (2018).

29. Abbott, B. P., et al. Multi-messenger Observations of a Binary Neutron Star Merger. *Astrophys. J. Lett.*, **848**, L12 (2017).
30. Ligo Scientific Collaboration, VIRGO Collaboration, & Kagra Collaboration GRB 231115A: Non-detection in low-latency of gravitational waves with LIGO/Virgo/KAGRA. *GRB Coordinates Network*, **35049**, 1 (2023).
31. Leroy, A. K., et al. A $z = 0$ Multiwavelength Galaxy Synthesis. I. A WISE and GALEX Atlas of Local Galaxies. *Astrophys. J. Supp.*, **244**, 24 (2019).
32. Duncan, R. C., & Thompson, C. Formation of Very Strongly Magnetized Neutron Stars: Implications for Gamma-Ray Bursts. *Astrophys. J. Lett.*, **392**, L9 (1992).
33. Cehula, J., Thompson, T. A., & Metzger, B. D. Dynamics of baryon ejection in magnetar giant flares: implications for radio afterglows, r-process nucleosynthesis, and fast radio bursts. *arXiv e-prints*, arXiv:2311.05681 (2023).
34. Frederiks, D. D., et al. Giant flare in SGR 1806-20 and its Compton reflection from the Moon. *Astronomy Letters*, **33**, 1 (2007).
35. Mereghetti, S., et al. The First Giant Flare from SGR 1806-20: Observations Using the Anticoincidence Shield of the Spectrometer on INTEGRAL. *Astrophys. J. Lett.*, **624**, L105 (2005).

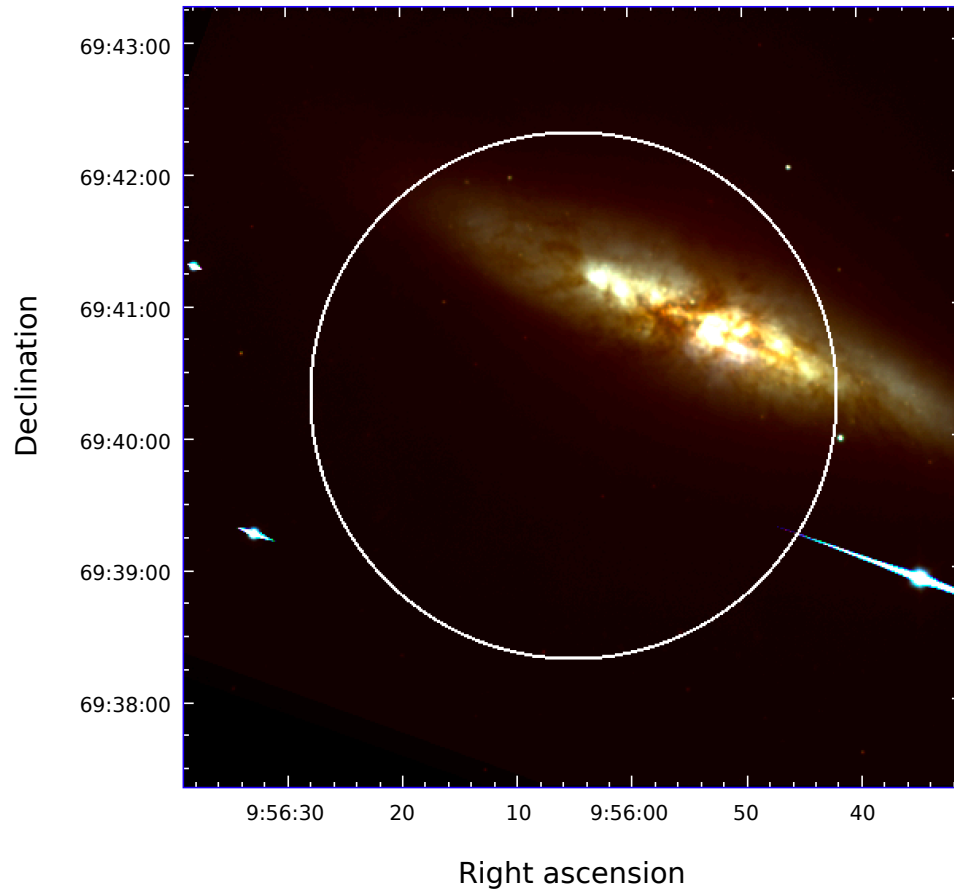


Figure 1: **Optical image of M82** (from data obtained with the TNG). RGB scale: z-band (red), i-band (green), r-band (blue). The 90% c.l. error circle of GRB 231115A has a radius of 2 arcmin.

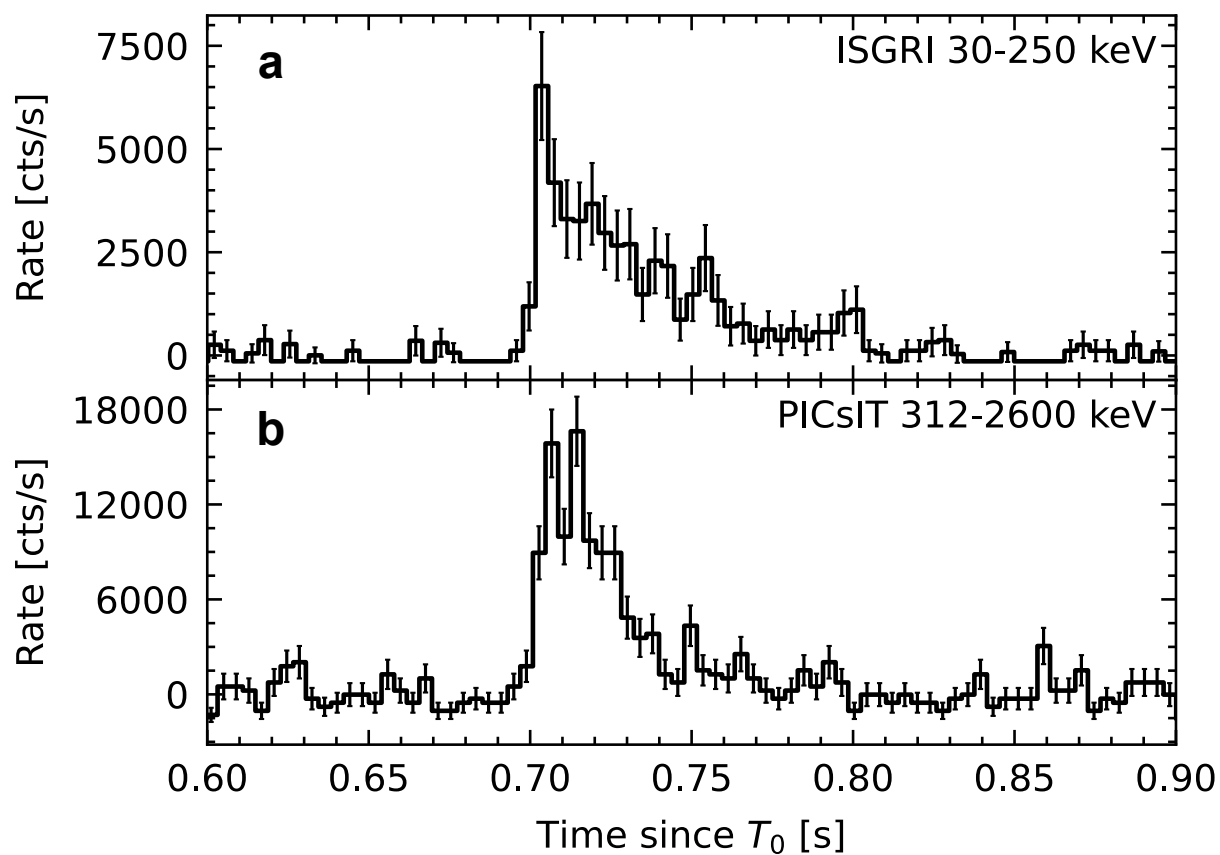


Figure 2: **Light curves of GRB 231115A.** Background-subtracted light curves (errors are at 1σ) obtained with the ISGRI detector in the 30–250 keV energy range (a) and with the PICsIT detector in the 312 – 2600 keV energy range (b). Time is referred to $T_0 = 2023-11-15\ 15:36:20$ UT (time at the *INTEGRAL* position; the burst reached instruments on low Earth orbit satellites about 0.4 s later).

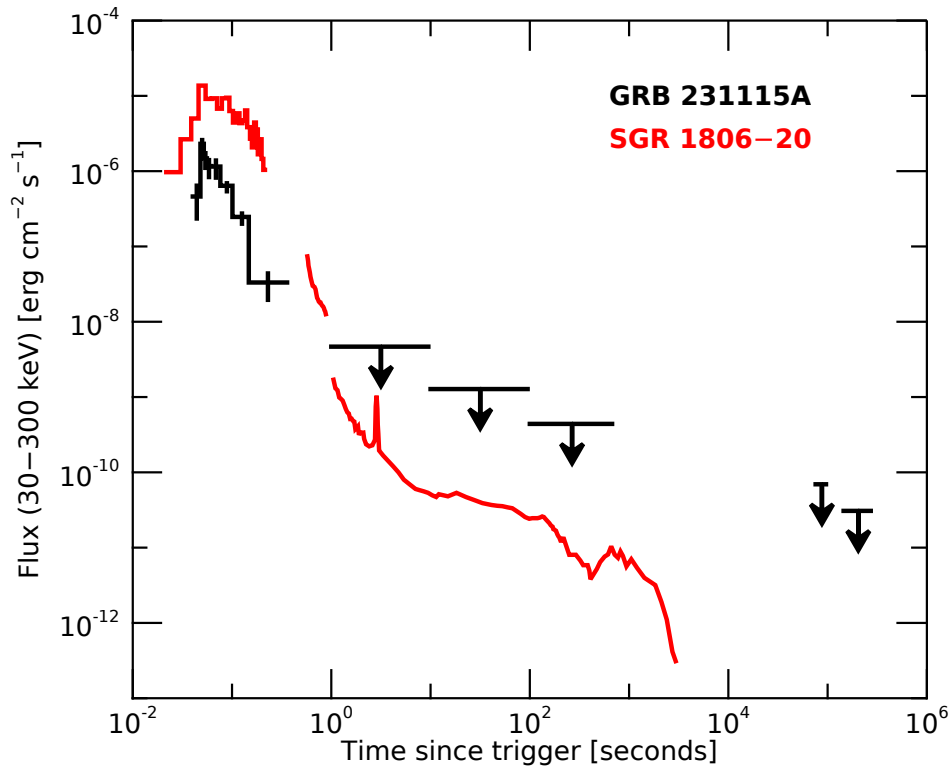


Figure 3: **Comparison between GRB 231115A and the 2004 giant flare from SGR 1806–20.** Errors are at 1σ , upper limits are at 3σ . The light curve of SGR 1806–20 (red) has been rescaled to the distance of M82 (data from Helicon-Coronas-F³⁴, Konus-Wind³⁴ and *INTEGRAL* SPI-ACS³⁵). Note that the 5.2 s periodicity in the SGR 1806–20 light curve is not visible due to the used bin size.

Methods

1 *INTEGRAL* data analysis and results

IBIS is a γ -ray telescope based on two position-sensitive detection planes working in different overlapping energy ranges: ISGRI²² (20 keV – 1 MeV) and PICsIT²³ (175 keV – 15 MeV). A coded mask placed about 3.2 m above ISGRI provides imaging capabilities over a field of view of $\sim 30 \times 30$ deg². GRB 231115A was detected at an off-axis angle of 4°, inside the fully coded field of view. For the data reduction and analysis, we used version 11.2 of the Offline Science Analysis (OSA) software³⁶, with the most recent calibration files, that properly account for the time evolution of the instrument response.

Burst spectrum We extracted an ISGRI spectrum, in 14 logarithmically spaced energy channels between 30 – 500 keV, for the time interval from 15:36:20.687 to 15:36:20.748 UT. The PICsIT spectrum for the same time interval was extracted from the spectral-timing data mode in 8 predefined energy channels spanning 212 – 2600 keV. Data in spectral-timing mode (counts integrated over the whole detector in 3.9 ms time bins) do not provide imaging information (contrary to the ISGRI data). Therefore, the background count-rate in each PICsIT energy channel was calculated as the median count rate during the *INTEGRAL* pointing (5013 s duration) containing the burst. A proper correction factor was applied to the PICsIT effective area to account for the angular distance between the IBIS pointing direction and GRB 231115A.

We added 5% systematic uncertainties to both spectra. The ISGRI and PICsIT spectra were fitted simultaneously using XSPEC³⁷ version 12.12.1. A fit with a power law was unacceptable ($\chi^2 = 59.4$ for 17 degrees of freedom), while a power law with exponential cut-off, defined as $F(E) = KE^\alpha \exp(-E(2 + \alpha)/E_p)$, gave a good fit with photon index $\alpha = 0.04_{-0.24}^{+0.27}$, peak energy $E_p = 551_{-59}^{+81}$ keV, and 30 – 2600 keV flux $F = (7.2 \pm 0.6) \times 10^{-6}$ erg cm⁻² s⁻¹.

The ISGRI spectrum for the time interval corresponding to the whole GRB, from 15:36:20.687 UT to 15:36:20.833 UT, is less well constrained, but the best fit parameters are within the errors consistent with those of the ISGRI plus PICsIT spectrum. All the fit parameters are summarized in Table 1, where we give also the results obtained with a blackbody model.

Follow up observation. Immediately after the discovery of GRB 231115A we requested an *INTEGRAL* Target of Opportunity (ToO) observation that started only 21 hours after the burst and continued

in the next satellite revolution. The first part of the ToO was done between 12:38 UT and 19:46 UT of November 16. The next one from 07:21 UT of November 17 to 23:09 UT of November 18, resulting in a total exposure of 162 ks divided in 57 pointings. Using the OSA 11.2 software, we produced the mosaics of the ISGRI images in the 30 – 100 keV energy range for three periods: November 16, November 17-18, and November 16 to 18. No sources were detected at the position of GRB 231115A. The $3\text{-}\sigma$ upper limits on the 30 – 100 keV flux, derived assuming a thermal bremsstrahlung spectrum with temperature $kT = 30$ keV, are 6.5×10^{-11} erg cm $^{-2}$ s $^{-1}$ for November 16, 2.9×10^{-11} erg cm $^{-2}$ s $^{-1}$ for November 17-18, and 2.6×10^{-11} erg cm $^{-2}$ s $^{-1}$ for the sum of the two periods. We also derived an upper limit of 3.8×10^{-10} erg cm $^{-2}$ s $^{-1}$ on the flux in the time interval from $T_0 + 1.7$ s to $T_0 + 11.8$ min, during which the GRB 231115A position was in the IBIS field of view. All these upper limits are plotted in Figure 3, where it can be seen that, even a giant flare as energetic as the one emitted from SGR 1806–20, at the distance of M82 would have been undetectable by IBIS after the initial bright pulse.

Search for past activity from M82. The region of M82 has been repeatedly observed with *INTEGRAL*, starting in November 2003. After eliminating the time intervals with strong and variable background (typically due to solar activity or to particles trapped in the Earth radiation belts when the satellite is close to perigee) we obtained about 16 millions of seconds of useful time with M82 in the IBIS field of view. We extracted ISGRI lightcurves in the 30 – 150 keV energy range, using only detector pixels illuminated for more than 50% from a source at the GRB 231115A position and searched for excess counts in the light curves over eight logarithmically spaced timescales between 0.01 and 1.28 s (see ³⁸ for more details). All the burst candidates found in the light curves were then examined by making the sky images of the corresponding time intervals. None of them showed the presence of a source at the M82 position. Through simulations we found that bursts down to a factor ~ 5 fainter than GRB 231115A would have been detected in these data, assuming the same time profile and spectrum.

2 X-ray observations

Swift pointed at M82, starting to collect data 9.0 ks after the burst occurrence²⁵. *Swift*/XRT observations were carried out in Photon Counting mode in the 9.0–39.2 ks time interval, collecting 4.4 ks of data. No new X-ray sources were detected within the *INTEGRAL* error region of GRB 231115A. The $3\text{-}\sigma$ upper limit is position-dependent due to the diffuse X-ray emission from the M82 galaxy. Outside the galaxy, the upper limit on the count rate is $\sim 2 - 3 \times 10^{-3}$ counts

s^{-1} . Assuming a power-law spectrum with photon index $\Gamma = 2$ and the Galactic column density of $6.5 \times 10^{20} \text{ cm}^{-2}$ (the total Galactic absorption column in the line of sight of M82³⁹) this corresponds to a 0.3 – 10 keV unabsorbed flux of $\sim 10^{-13} \text{ erg cm}^{-2} \text{ s}^{-1}$.

A 47 ks long ToO observation of GRB 231115A was carried out with the *XMM-Newton* satellite, starting on 2023 November 16 at 08:29:16 UT, about 16.9 hours after the burst (Obs.ID 093239)²⁶. The EPIC-pn⁴⁰ and the two EPIC-MOS⁴¹ cameras were operated in Full window mode, with the thin optical-blocking filter. We processed the data with the EPPROC and EMPROC pipelines of version 18 of the Science Analysis System (SAS)⁴² and the most recent calibration files and selected the EPIC events with standard filtering expressions. Time intervals of high background were removed with the ESPFILT task with standard parameters, thus yielding net exposure times of 7.56 ks (pn), 18.78 ks (MOS1) and 23.41 ks (MOS2). We selected single- and multiple-pixel events (PATTERN ≤ 4 for the pn and ≤ 12 for the MOS cameras); out-of-time events were also removed following the standard procedure^a.

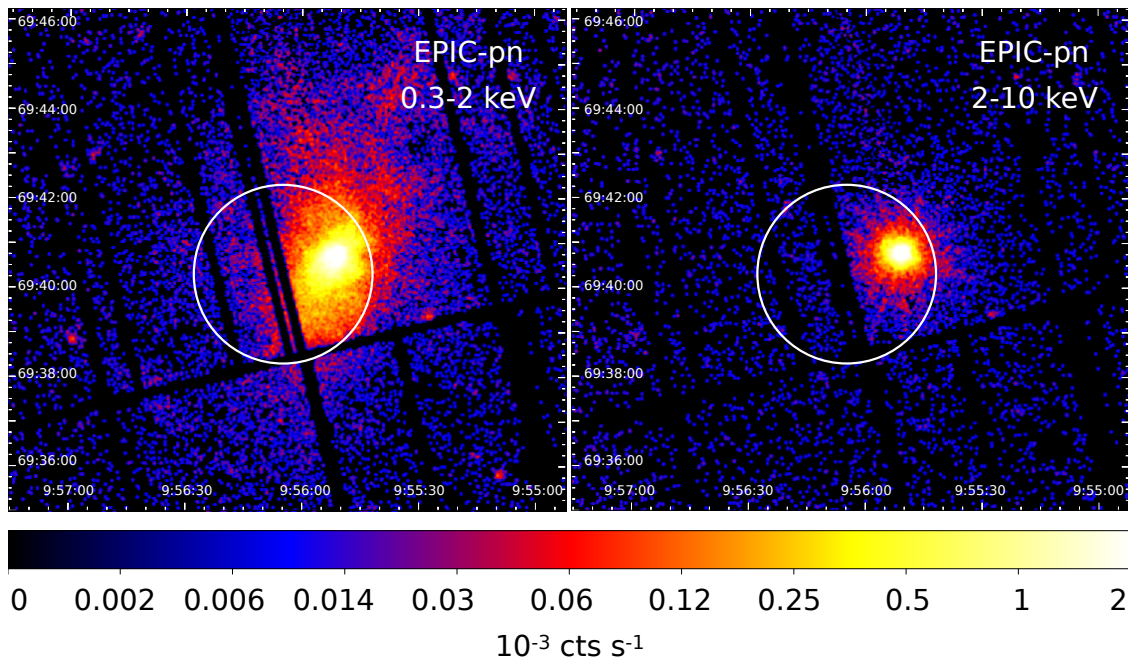


Figure 4: **EPIC-pn images of M82**. The exposure-corrected images refer to the 0.3 – 2 keV (a) and 2 – 10 keV (b) energy ranges. The 90% c.l. error circle of GRB 231115A has a radius of 2 arcmin.

^a<http://www.cosmos.esa.int/web/xmm-newton/sas-thread-epic-oot>

Figure 4 shows the pn exposure-corrected images in the soft (0.3 – 2 keV) and hard (2 – 10 keV) energy ranges. The images are dominated by the diffuse X-ray emission of the M82 galaxy, especially in the soft X-ray band. We compared the images obtained in this observation with those of all the previous pointings on M82 available in the *XMM-Newton* archive (Obs.ID 011229, 020608, 056059, 065780, 087094, 089106). We did not find any evidence for the appearance of a new source. In our observation, the total emission between 2 – 10 keV from a circular region of radius 1.5 arcmin at the center of the galaxy (coordinates R.A. = 09^h 55^m 50^s.9, Dec. = +69° 40' 47"; J2000) can be described by an absorbed power law with $N_{\text{H}} = (1.0 \pm 0.1) \times 10^{22} \text{ cm}^{-2}$, photon index $\Gamma = 2.01 \pm 0.04$ and unabsorbed flux $F_{2-10 \text{ keV}} = (2.88 \pm 0.04) \times 10^{-11} \text{ erg cm}^{-2} \text{ s}^{-1}$. The flux measured in previous *XMM-Newton* observations from the same extraction region and the same spectral model varied between $\sim 1.2 \times 10^{-11} \text{ erg cm}^{-2} \text{ s}^{-1}$ and $\sim 5.4 \times 10^{-11} \text{ erg cm}^{-2} \text{ s}^{-1}$, indicating the presence of one or more variable sources that cannot be individually resolved with the *XMM-Newton* spatial resolution.

To compute the upper limit for a new point source in the GRB 231115A error box, we applied the EUPPER task to the 2 – 10 keV images. We used a circle of radius 15'' for the source extraction and a concentric annulus of radii 22.5'' and 30'' for the background. The derived upper limits have been corrected for the fraction of source counts falling outside the extraction circle. Figure 5 shows the 3- σ upper limits obtained by applying this procedure on a grid of positions with a step of 5''.

We used the appropriate EPIC response matrices to convert the count rates of each camera to fluxes in the 0.3 – 10 keV and 2 – 10 keV energy ranges, with the assumption of an absorbed power-law spectrum with photon index $\Gamma = 2$ and $N_{\text{H}} = 6.5 \times 10^{20} \text{ cm}^{-2}$. Finally we combined the upper limits of the three cameras to obtain an EPIC upper limit for each energy band. The results are shown in Figure 6. About 60% of the error circle has a 3- σ upper limit of $F_{2-10 \text{ keV}} = 1.2 \times 10^{-14} \text{ erg cm}^{-2} \text{ s}^{-1}$ and $F_{0.3-10 \text{ keV}} = 4.0 \times 10^{-14} \text{ erg cm}^{-2} \text{ s}^{-1}$. In less than 10% of the error circle, the upper limit is worse than $7 \times 10^{-14} \text{ erg cm}^{-2} \text{ s}^{-1}$ (2 – 10 keV) and $1.6 \times 10^{-13} \text{ erg cm}^{-2} \text{ s}^{-1}$ (0.3 – 10 keV). At the distance of M82, these fluxes correspond to luminosities of 1.9×10^{36} and $6.2 \times 10^{36} \text{ erg s}^{-1}$, respectively.

Figure 7 shows the comparison between the X-ray light curves of short GRBs (defined such as $T_{90} \leq 2 \text{ s}$), obtained from the *Swift* GRB catalog^b and the 3- σ upper limits we derived from the *Swift* and *XMM-Newton* observations of GRB 231115A.

^bhttp://swift.gsfc.nasa.gov/archive/grb_table

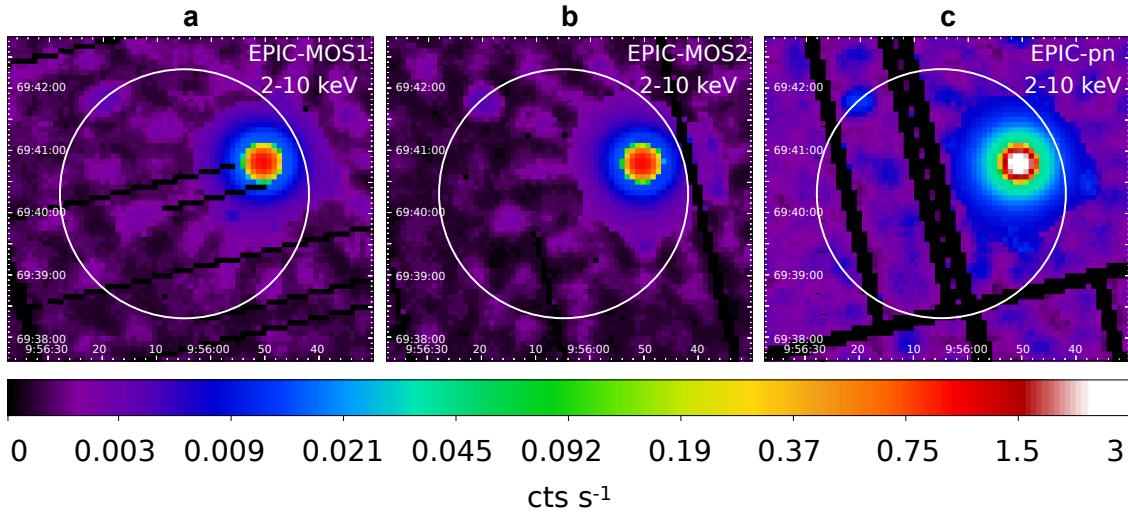


Figure 5: **Maps of count rate upper limits.** The figure gives $3\text{-}\sigma$ upper limits on the 2 – 10 keV count rates of the EPIC-MOS1 (a), EPIC-MOS2 (b) and EPIC-pn (c) cameras. The 90% c.l. error circle of GRB 231115A has a radius of 2 arcmin.

3 Optical observations

Multi-filter follow-up optical observations of GRB 231115A were carried out with the wide-field Schmidt telescopes sited in INAF observatories of Padova (Asiago, Italy), Abruzzo (Campo Imperatore, Italy) and with the 3.6-m Telescopio Nazionale Galileo (TNG, Canary Islands, Spain) between about 5 and 12 hours from the event T_0 . We also took additional VRI images about 7 hours after T_0 with the 120 cm Newton telescope located at the Observatoire de Haute Provence (OHP, France). The log of the observations is reported in Table 2. Image reduction was carried out following the standard procedures: subtraction of an averaged bias frame and division by a normalized flat frame. Astrometry was performed using the Pan-STARRS^c catalogue. We carried out image subtraction with respect to SDSS^d and telescope archival templates using the *HOTPANTS* (High Order Transform of Psf ANd Template Subtraction code⁴³) package to find and pinpoint variable sources within the *INTEGRAL* error circle. Aperture and PSF-matched photometry were performed

^c<http://outerspace.stsci.edu/display/PANSTARRS/>

^d<http://www.sdss.org>

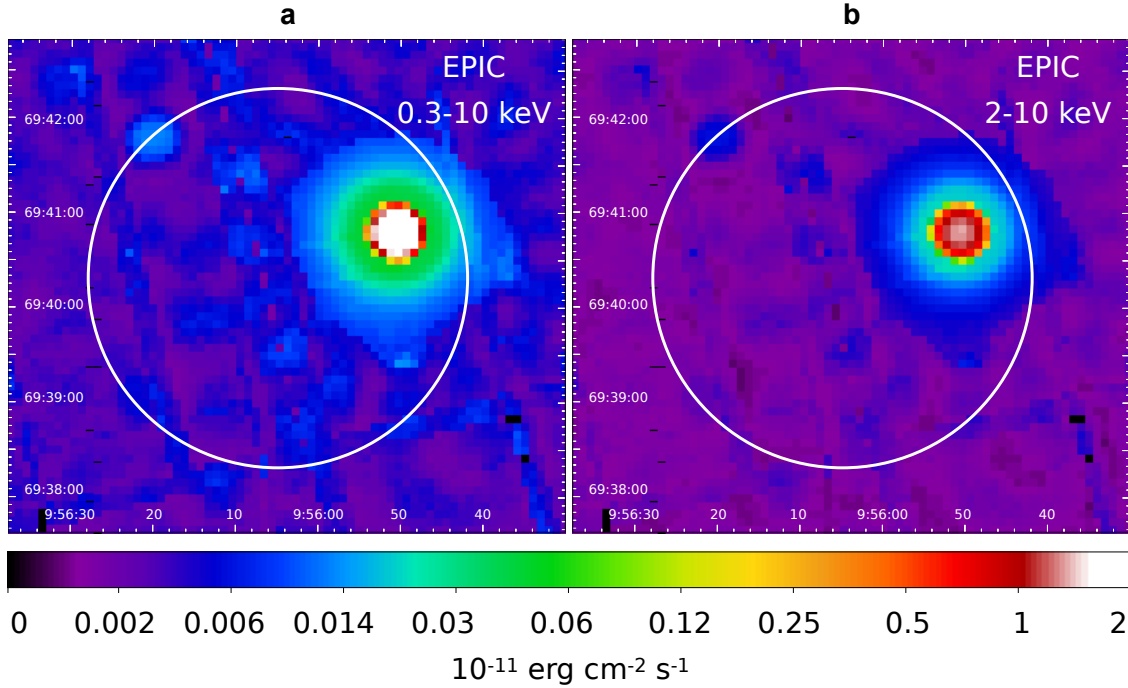


Figure 6: **Maps of flux upper limits.** The figure gives $3\text{-}\sigma$ upper limits on the fluxes in the 2 – 10 keV (a) and 0.3 – 10 keV (b) energy range, obtained by combining the three maps of ???. The 90% c.l. error circle of GRB 231115A has a radius of 2 arcmin.

using the DAOPHOT package⁴⁴ and the STDPIPE⁴⁵ and the PHOTUTILS^{e 46} packages for OHP/T120 images. To minimize any systematic effect, we performed differential photometry with respect to a selection of local isolated and non-saturated reference stars from the Pan-STARRS^f. The presence of the M82 galaxy makes the background highly non-uniform within the *INTEGRAL* error circle. Magnitude upper limits have been computed for two regions (see Table 2): one (most conservative) corresponding to the centre of the M82 galaxy (R.A. = $09^{\text{h}} 55^{\text{m}} 53^{\text{s}}.75$, Dec. = $+69^{\circ} 40' 53''.9$; J2000) and another outside the core of the galaxy light (R.A. = $09^{\text{h}} 56^{\text{m}} 11^{\text{s}}.31$, Dec. = $+69^{\circ} 39' 09''.6$; J2000).

Our upper limits in the optical bands (Table 2) exclude the majority of cosmological short GRB afterglows. If occurred at the distance of M82, in a position located inside (outside) the galaxy, a short GRB would have produced an optical afterglow more than 12 (16) magnitudes

^e<http://github.com/astropy/photutils>

^f<http://outerspace.stsci.edu/display/PANSTARRS/>

Table 1: **Results of spectral fits of GRB 231115A.** Errors are at 1σ , fluxes are in the 30 – 2600 keV energy range. Time intervals are in seconds after $T_0 = 15:36:20$ UT.

Detectors	ISGRI+PICsIT	ISGRI
Time interval	0.687–0.748	0.687–0.833
Blackbody		
kT (keV)	108_{-5}^{+7}	68_{-11}^{+12}
Flux (10^{-6} erg cm $^{-2}$ s $^{-1}$)	$7.9_{-0.7}^{+0.6}$	$2.1_{-0.7}^{+0.6}$
χ^2 / d.o.f.	31.9/17	16.4/12
Cut-off power law		
α	$0.04_{-0.24}^{+0.27}$	$0.55_{-0.42}^{+0.50}$
E_p (keV)	551_{-59}^{+81}	355_{-89}^{+158}
Flux (10^{-6} erg cm $^{-2}$ s $^{-1}$)	$7.2_{-0.7}^{+0.6}$	2.7 ± 1.1
χ^2 / d.o.f.	17.2/16	14.9/11

Table 2: **Log of optical observations of GRB 231115A.** Magnitudes are in the AB system, not corrected for Galactic extinction. Upper limits are given at $3\text{-}\sigma$ confidence level for a source within (outside) the M82 galaxy.

UT observation (start - stop)	Exposure (s)	T - T_0 (days)	Telescope	Magnitude	Filter
2023-11-15 20:40:03 - 20:54:15	5×180 s	0.211	Asiago	$> 19.1(> 20.1)$	<i>g</i>
2023-11-15 20:54:59 - 21:12:11	5×180 s	0.221	Asiago	$> 19.0(> 20.1)$	<i>r</i>
2023-11-15 21:12:45 - 21:27:45	5×180 s	0.234	Asiago	$> 18.3(> 19.8)$	<i>i</i>
2023-11-15 21:38:00 - 22:16:30	7×300 s	0.251	Campo Imperatore	$> 14.8(> 18.9)$	<i>z</i>
2023-11-15 22:38:25 - 21:31:30	9×300 s	0.293	Campo Imperatore	$> 16.5(> 19.8)$	<i>i</i>
2023-11-15 23:33:32 - 21:38:00	7×300 s	0.331	Campo Imperatore	$> 18.8(> 20.7)$	<i>g</i>
2023-11-15 22:35:32 - 22:57:23	1×1400 s	0.299	OHP	$> 17.3(> 21.6)$	<i>r</i>
2023-11-15 23:04:02 - 23:14:02	1×600 s	0.314	OHP	$> 18.0(> 22.0)$	<i>g</i>
2023-11-15 23:14:30 - 23:19:30	1×300 s	0.320	OHP	$> 17.1(> 20.1)$	<i>i</i>
2023-11-16 03:25:04 - 03:38:16	5×120 s	0.492	TNG	$> 20.0(> 24.0)$	<i>r</i>
2023-11-16 03:40:24 - 03:59:09	7×120 s	0.503	TNG	$> 18.9(> 23.8)$	<i>i</i>
2023-11-16 04:00:28 - 04:19:17	7×120 s	0.530	TNG	$> 18.7(> 22.7)$	<i>z</i>

brighter than our limits (see Fig. 9). These upper limits are about 9 (13) magnitudes fainter than the expected brightness of a kilonova like AT2017gfo occurring at the distance of M82 inside (outside) the galaxy. Since kilonovae associated to short GRBs can display significant differences in their luminosity, spectral properties, and temporal evolution⁴⁷, we simulated a set of light curves with the POSSIS code⁴⁸ using the parameter range reported in⁴⁹. We found that even the faintest event, placed at the distance of M82, is still about 5 (9) magnitudes brighter than our upper limits.

References

36. Goldwurm, A., et al. The INTEGRAL/IBIS scientific data analysis. *Astron. Astrophys.*, **411**, L223 (2003).
37. Arnaud, K. A. XSPEC: The First Ten Years. *Astronomical Data Analysis Software and Systems V*, **101**, 17 (1996).
38. Mereghetti, S., Topinka, M., Rigoselli, M., & Götz, D. INTEGRAL Limits on Past High-energy Activity from FRB 20200120E in M81. *Astrophys. J. Lett.*, **921**, L3 (2021).
39. HI4PI Collaboration, et al. HI4PI: A full-sky H I survey based on EBHIS and GASS. *Astron. Astrophys.*, **594**, A116 (2016).
40. Strüder, L., et al. The European Photon Imaging Camera on XMM-Newton: The pn-CCD camera. *Astron. Astrophys.*, **365**, L18 (2001).
41. Turner, M. J. L., et al. The European Photon Imaging Camera on XMM-Newton: The MOS cameras. *Astron. Astrophys.*, **365**, L27 (2001).
42. Gabriel, C., et al. The XMM-Newton SAS - Distributed Development and Maintenance of a Large Science Analysis System: A Critical Analysis. *Astronomical Data Analysis Software and Systems (ADASS) XIII*, **314**, 759 (2004).
43. Becker, A. HOTPANTS: High Order Transform of PSF ANd Template Subtraction. *Astrophysics Source Code Library*, ascl:1504.004 (2015).
44. Stetson, P. B. DAOPHOT: A Computer Program for Crowded-Field Stellar Photometry. *Pub. Ast. Soc. Pac.*, **99**, 191 (1987).

45. Karpov, S. STDPipe: Simple Transient Detection Pipeline. *arXiv e-prints*, arXiv:2112.006 (2021).
46. Bradley, L., Sipőcz, B. Robitaille, T., et al. astropy/photutils: 1.1.0, *Zenodo*, 10.5281/zenodo.4624996 (2021).
47. Rossi, A., et al. A comparison between short GRB afterglows and kilonova AT2017gfo: shedding light on kilonovae properties. *Mon. Not. R. Astron. Soc.*, **493**, 3379 (2020).
48. Bulla, M. POSSIS: predicting spectra, light curves, and polarization for multidimensional models of supernovae and kilonovae. *Mon. Not. R. Astron. Soc.*, **489**, 5037 (2019).
49. Ferro, M., et al. A search for the afterglows, kilonovae, and host galaxies of two short GRBs: GRB 211106A and GRB 211227A. *Astron. Astrophys.*, **678**, A142 (2023).

Acknowledgements We thank the ESA Mission Scientists Jan-Uwe Ness and Norbert Schartel for approving and quickly implementing the *INTEGRAL* and *XMM-Newton* ToO observations. This work is based on observations with *INTEGRAL* and *XMM-Newton*, ESA missions with instruments and science data centres funded by ESA member states, and with the participation of the Russian Federation and the USA. It is also based on observations made with the Italian Telescopio Nazionale Galileo (TNG) operated on the island of La Palma by the Fundación Galileo Galilei of the INAF (Istituto Nazionale di Astrofisica) at the Spanish Observatorio del Roque de los Muchachos of the Instituto de Astrofisica de Canarias. This paper includes optical data taken with the Schmidt 67/92 telescope operated by INAF Osservatorio Astronomico di Padova (Mt. Ekar, Asiago). This work received financial support from INAF through the Magnetars Large Program Grant (PI S.Mereghetti) and from the GRAWITA Large Program Grant (PI P. D’Avanzo). JCR, AB, SM and PU acknowledge financial support from ASI under contract n. 2019-35-HH.0. FO acknowledges support from MIUR, PRIN 2020 (grant 2020KB33TP) “Multimessenger astronomy in the Einstein Telescope Era (METE).

Authors contributions All authors reviewed the manuscript and contributed to the source interpretation. SM coordinated the work and the interpretation of the results, contributed to the analysis of the *INTEGRAL* and *XMM-Newton* data, and wrote most of the manuscript. RS and EA contributed to write the main part of the paper. DP and JCR carried out most of the *INTEGRAL* data analysis. DG, CF, EB, LD and VS routinely contribute to the operation of the IBAS software and participated to the near real time *INTEGRAL* analysis. PDA coordinated the analysis of the optical data from Italian telescopes. MR analysed the *XMM-Newton* data and contributed to the *INTEGRAL* spectral analysis. SC analysed the *Swift* data. MT contributed to the

software for the burst search in archival data. DT, WT and CA coordinated the observation and the analysis of the optical data taken at OHP. LT analysed the optical data taken with the Schmidt 67/92 telescope in Asiago under the Large Program "Search and characterisation of optical counterparts of GW triggers" (P.I. Tomasella). AR and EC triggered, reduced and analysed the observations at the Asiago Schmidt telescope. RB and MF provided the short GRB afterglows and kilonovae observed and simulated optical light curves.

Competing Interests The authors declare no competing interests.

Correspondence Correspondence and requests for materials should be addressed to Sandro Mereghetti (email: sandro.mereghetti@inaf.it).

Data Availability The data of the INTEGRAL, *XMM-Newton* and *Swift* satellites are publicly available in the respective online archives

(<https://www.isdc.unige.ch/integral/archive>,

<https://www.cosmos.esa.int/web/xmm-newton/xsa>,

<https://swift.gsfc.nasa.gov/archive/>)

. Optical data are available upon reasonable request.

Code Availability The software used for the data analysis is public and can be retrieved at

<https://www.cosmos.esa.int/web/xmm-newton/sas>,

<https://www.isdc.unige.ch/integral/analysis> Software,

<https://heasarc.gsfc.nasa.gov/xanadu/xspec/>

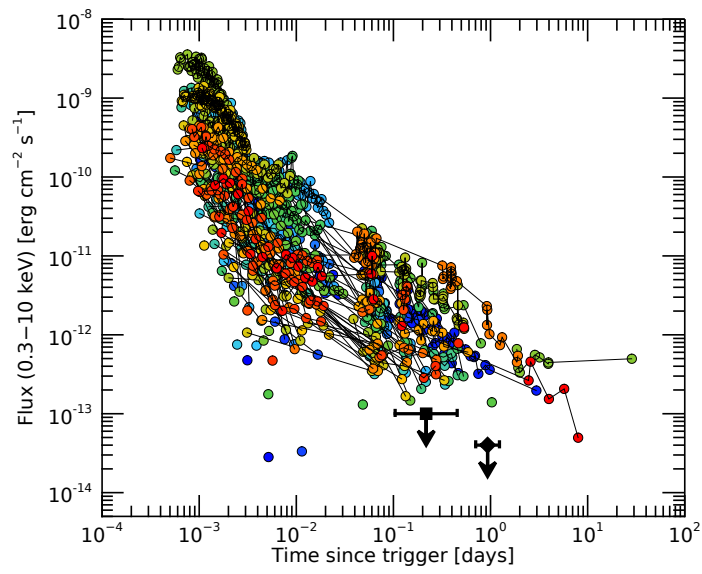


Figure 7: **X-ray light curves of short GRB afterglows.** The *Swift*/XRT (black square) and *XMM-Newton*/EPIC (black diamond) $3\text{-}\sigma$ upper limits of GRB 231115A are indicated.

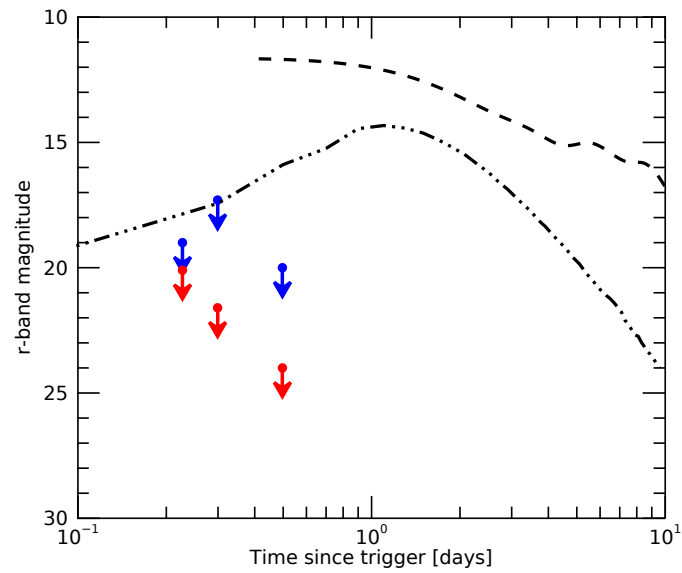


Figure 8: **Optical light curves of kilonovae.** The r-band light curves of AT2017gro and of the faintest red kilonova (simulated with the POSSIS code) are shown with dashed and dashed-dotted lines, respectively, assuming the M82 distance (3.6 Mpc). The magnitude $3\text{-}\sigma$ upper limits obtained for a position inside (outside) the M82 galaxy are shown as blue (red) arrows.

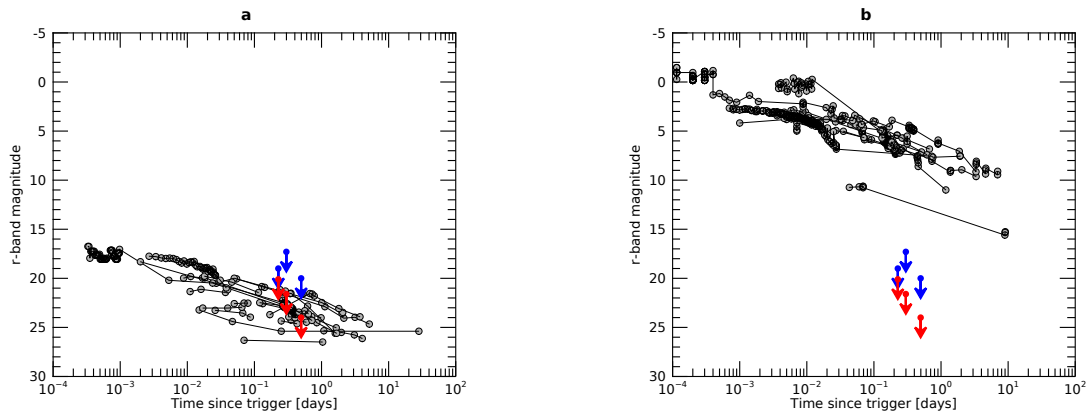


Figure 9: **Optical light curves of short GRB afterglows.** The observed light curves are shown in **a**, while **b** shows the light curves of those GRBs which have a measure of redshift, rescaled to the M82 distance (3.6 Mpc). The $3\text{-}\sigma$ upper limits obtained for a position inside (outside) the M82 galaxy are shown as blue (red) arrows.